

Methylene Blue and Malachite Green Removal From Aqueous Solution Using Waste Activated Carbon

Sneha Prabha Mishra ^{1,*}, Amiya Ranjan Patra ¹, Shubhalaxmi Das ¹

¹ Department of Chemistry, Siksha 'O' Anusandhan (Deemed to Be University), Bhubaneswar, 751 030, India

* Correspondence: spm_iter@rediffmail.com;

Scopus Author ID 57211529060

Received: 19.05.2020; Revised: 11.06.2020; Accepted: 12.06.2020; Published: 16.06.2020

Abstract: In the present investigation, Waste Activated Carbon (WAC) collected from domestic water filter has been used for the removal of two cationic dyes methylene blue (MB) and malachite green (MG) from synthetic solution. The surface of WAC is characterized to know the mechanism of adsorption reaction and the effect of different adsorption parameters like pH, temperature, contact period, adsorbate and adsorbent doses are also studied for the said adsorption study. The optimum contact times for MB and MG adsorption on WAC are 60 and 120 minutes respectively, whereas pH is having no significant effect on adsorption. However, % adsorption increases slowly with the increase of pH from 2.5 to 7. Adsorption of both the dyes on WAC is exothermic, spontaneous, and favorable in nature. Langmuir isotherm and pseudo-second-order kinetics are obeyed well. Langmuir's maximum monolayer adsorption capacities are found to be 15.38 and 18.87mg/g for MB and MG, respectively. Temkin isotherm, and Morris-Weber equations are also obeyed well. Temkin's isotherm concludes the physicochemical nature of adsorption, and Morris Weber equation indicates possibilities of intraparticle diffusion. The interaction between these two cationic dyes and WAC can be explained through electrostatic force of attraction or by hydrogen bonding.

Keywords: Methylene blue; malachite green; waste activated carbon; adsorption capacity; adsorption isotherm; intraparticle diffusion.

© 2020 by the authors. This article is an open-access article distributed under the terms and conditions of the Creative Commons Attribution (CC BY) license (<https://creativecommons.org/licenses/by/4.0/>).

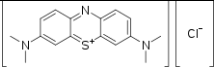
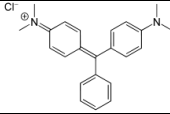
1. Introduction

Dye industries discharge colored water to the water bodies, which causes water pollution. Presently, more than one lakh synthetic dyes are available whose production over the year is 7×10^5 tonnes [1]. Water quality is recognized primarily by its color. The presence of even a very low concentration of dye (< 1 ppm) also results in an undesirable color of the water. Among the various dyes, azo dyes are most commonly used, and it accounts for the 60 – 70% of the total dye production [2]. Methylene blue (MB) is an azo dye that is commonly used for the coloring of silk, cotton, and wood. Its presence in the water causes several health disorders like eye burn, permanent injury to the human and animal eyes. It also causes breathing problems with a burning sensation. It may also cause mental confusion, metha moglobinemia, vomiting, nausea, and profuse sweating, etc. [3]. Similarly, Malachite green (MG) is another azo dye that is also used for coloring cotton, paper, jute, silk, wool, acrylic, and leather products. It is also used for coloring food agents, food additives, medicinal disinfectants, commercial fish hatching industries, and many more. Its presence in water also causes several

health injuries like damage to the nervous system, brain, liver, spleen, kidney, and heart. It also acts as a respiratory enzyme poison [4].

Dye concentration from the aqueous solution can be reduced by different treatment methods. These are sonochemical and photocatalytic degradation, cation exchange membranes, electrochemical degradation, solar photo-Fenton, and biological processes. These traditional methods cannot remove synthetic dyes from water and wastewater effectively [5]. Adsorption is a method that is considered simple, efficient, and economical for dye removal [6]. In the adsorption method, varieties of materials, either natural or synthetic, can be used as adsorbents [7]. However, carbon and its compounds are widely used for purification of various water sources as these adsorbents have a vast network of internal pores with the high surface area. So, these are considered as universal adsorbents [8]. Different carbon wastes are also reported to act as excellent adsorbents by a number of researchers [9,10]. The use of waste carbon and other waste materials for decontamination of polluted water is preferred because of its cost-effectiveness. Therefore, vast research is being carried out for the removal of various contaminants from aqueous solutions using different wastes, including carbon. MB and MG have also been tried widely for their removal by various low-cost adsorbents. The selection of suitable adsorbents for the removal of dyes is greatly dependent on the physicochemical characteristics of dyes. Dyes are generally classified based on their structural variation and application to the fabric. The physicochemical characteristics of MB and MG are given below in Table 1 [11,12].

Table 1. Physicochemical characteristics of both the dyes.

Parameters	Methylene Blue (MB)	Malachite Green (MG)
Molecular formula	C ₁₆ H ₁₈ ClN ₃ S	C ₂₃ H ₂₅ ClN ₂ (chloride)
Molecular weight	319.85 g/mol	364.911 g/mol (chloride)
IUPAC name	3,7-bis(Dimethylamino)-phenothiazin-5-ium chloride	4-[[4-(Dimethylamino)phenyl](phenyl)methylidene]-N,N-dimethylcyclohexa-2,5-dien-1-iminium chloride
Molecular structure		
Other names	Basic blue 9	Aniline green; Basic green 4; Diamond green B; Victoria green B
Maximum wavelength	670 nm	618nm

In the present investigation, removal of MG and MB from the synthetic aqueous solution has been tried with activated carbon collected after use as waste from the domestic water filter. The carbon used in a water filter is usually silver-impregnated activated carbon, which has been used earlier by Mishra and her coworkers for the removal of Cu(II) and Cr(VI) separately from aqueous solutions [13,14]. The main objective of this research article is (i) to carry out a detailed adsorption study for the removal of MB and MG by this waste activated carbon (WAC) varying different adsorption parameters (ii) characterization of the adsorbent and (iii) isotherms/kinetics interpretation of the data to find out the mechanism of adsorption.

2. Materials and Methods

2.1. Adsorbate and adsorbent.

A stock solution of 1000 g/L of each dye (MB and MG) was prepared separately by dissolving the required amount of dye in double-distilled water. The above stock solution was diluted to the desired concentrations required for various adsorption experiments. In domestic water filters, silver-impregnated activated carbon is used as water purifiers. It is prepared by activating coconut shell carbon at high temperatures in controlled conditions. After discarded from the water filters, it was collected, washed with deionized water several times, followed by oven drying at 100°C for two hours. Then these dried samples were kept in air prevented sample bottles for use.

2.2. Characterization of the adsorbents.

XRD (X-Ray Diffraction) of WAC was taken using Rigaku Ultima-IV X-Ray Diffractometer. JASCO FTIR instrument-4100 was used for FTIR (Fourier Transform Infrared) analysis using adsorbent:KBr pellet ratio of 1:100. The point of zero charge (pzc) was determined using the Solid addition method. The specific surface area of WAC was measured by BET (Brunauer-Emmett-Teller) method following the N₂ adsorption-desorption method by Micromeritics ASAP 2020 BET analyzer at 77K. The % moisture content and % mass loss on ignition were analyzed after keeping the required amount of WAC samples in the oven and furnace at 105°C and 600°C, respectively, for 2 hours each. The formula shown in equation 1 was used for the determination of both % mass loss and % moisture content.

$$\% \text{ mass loss or, \% moisture content} = \frac{W_2 - W_3}{W_2 - W_1} \times 100 \quad (1)$$

Where, W₁ - Weight of the empty crucible, g

W₂ - Weight of the sample with crucible before heating, g and

W₃ - Weight of the sample with crucible after heating, g.

The pH was determined to take 1g of adsorbent in 100ml of double-distilled water. After stirring for 1hr, the pH of the solution was measured using a pH meter. The density was measured by the water displacement method. The ratio between mass and displaced volume of water gives adsorbent density [14].

2.3. General procedure for batch adsorption study and analysis.

Various adsorption experiments were carried out batch-wise by constantly agitating the dye solution containing a fixed amount of WAC by magnetic stirrer maintained at a constant temperature. In most of the cases, 1g of the adsorbent was mixed with 50ml of dye solution. During adsorption experiments, samples were taken at different time intervals, and the concentration of MB and MG in the solution was determined by an Elico SL-244 double beam UV-Visible Spectrophotometer at wavelengths of 670 and 618nm respectively. The dye adsorption capacity of WAC was determined by using the formula

$$q = \frac{(C_o - C_e)V}{M} \quad (2)$$

$$\text{Sorption}(\%) = [(C_o - C_e)/C_o] \times 100 \quad (3)$$

Where, q - Dye concentration on the adsorbent surface at equilibrium, mg/g,

C_o - Initial dye concentration, mg/L

C_e - Dye concentration at equilibrium, mg/L

V - Volume of the solution, L and

M - Mass of the adsorbent, g.

2.4. Adsorption kinetics/isotherms.

In adsorption studies, kinetics/isotherm equations play an important role as it determines the rate and mechanism of the reaction. The mechanism of adsorption studies depends on the physical and chemical properties of both adsorbents and adsorbates. Therefore, following kinetics/isotherm equations mentioned in Table 2 are applied to adsorption data of MB and MG adsorption on WAC. The details of the kinetics/isotherm models are given in Table 2.

Table 2. Description of adsorption and kinetic equations.

Sl. no.	Models	Equations in linear form	Plots	Determination of the parameters
1	Langmuir isotherm	$C_e/q_e = 1/q_m b + C_e/q_m$	C_e in X axis C_e/q_e in Y axis	q_m from slope b from intercept
2	Freundlich isotherm	$\log q_e = \log K + 1/n \log C_e$	$\log C_e$ in X axis $\log q_e$ in Y axis	n from slope K from intercept
3	Temkin isotherm	$q_e = B \ln A_T + B \ln C_e$	$\ln C_e$ in X axis: q_e in Y axis:	B from slope A_T from intercept
4	Lagergren's pseudo 1 st order equation	$\log(q_e - q_t) = \log(q_e) - (k_1/2.303)t$	t in X axis $\log(q_e - q_t)$ in Y axis:	k_1 from slope q_e from intercept
5	Ho & Mc-Kay pseudo 2 nd order equation	$t/q_t = 1/k_2 q_e^2 + 1/q_e t$	t in X axis t/q_t in Y axis	q_e from slope k_2 from intercept
6	Morris-Weber equation	$q_t = R_{id} t^{1/2}$	$t^{1/2}$ in X axis: q_t in Y axis:	R_{id} from slope No intercept

Where,

- C_e - Dye concentration at equilibrium, mg/L
- q_e - Dye adsorbed per unit weight of WAC, mg/g at equilibrium
- q_m - Langmuir maximum adsorption capacity, mg/g
- b - Langmuir constant related to adsorption energy, L/mg
- K - Freundlich adsorption capacity, mg/g,
- n - Freundlich constant related to adsorption intensity
- q_t - Dye adsorbed on WAC, mg/g at any time t
- B - Temkin's adsorption heat, J/mg
- A_T - Temkin's equilibrium binding constant, L/mg
- k_1 - Rate constant for pseudo 1st order kinetics, 1/min.
- k_2 - Rate constant for pseudo 2nd order kinetics, g/mg/min
- R_{id} - Intra particle transport rate constant, mg/g/min^{0.5}

A dimensionless constant, i.e., Separation factor (R_L), can be determined from Langmuir constant b using equation (4) as follows.

$$R_L = 1/(1 + bC_0) \tag{4}$$

Where, C_0 - Initial concentration of dye, mg/L

When $R_L > 1$, the reaction is not favorable, when $R_L = 1$, the reaction is linear, $R_L = 0 - 1$ indicates favorable reaction and $R_L = 0$ indicates irreversible reaction [15].

2.5. Adsorption thermodynamics.

The van't Hoff equation was used to determine three thermodynamic parameters such as enthalpy change (ΔH), entropy change (ΔS), and free energy change (ΔG). The equation is

$$\ln K_D = \Delta S/R - \Delta H/RT \tag{5}$$

Where, K_D - Distribution coefficient = $\frac{\text{Adsorbate concentration on adsorbent } (\frac{mg}{g}) \text{ at equilibrium}}{\text{Adsorbate concentration in solution } (\frac{mg}{L}) \text{ at equilibrium}}$

T - Temperature, K

R - Universal gas constant, J/K/mol

So, ΔH and ΔS can be obtained from the slope and intercept respectively when $\ln K_D$ is plotted against $1/T$. Free energy change (ΔG) of specific adsorption is calculated from the equation as follows

$$\Delta G = \Delta H - T\Delta S \quad (6)$$

3. Results and Discussion

3.1. Characterization of WAC surface.

3.1.1. XRD analysis.

Figure 1 shows the XRD of WAC. Two remarkable peaks at $2(\theta) = 24$ and 44°C confirm the typical carbon structure of the adsorbent and represents (002) and (101) basal planes, respectively. It shows a typical graphite structure where three adjacent carbon atoms are bonded with the basal planes through covalent bonding. The basal planes are interconnected with each other by weak van der Waal's forces [16].

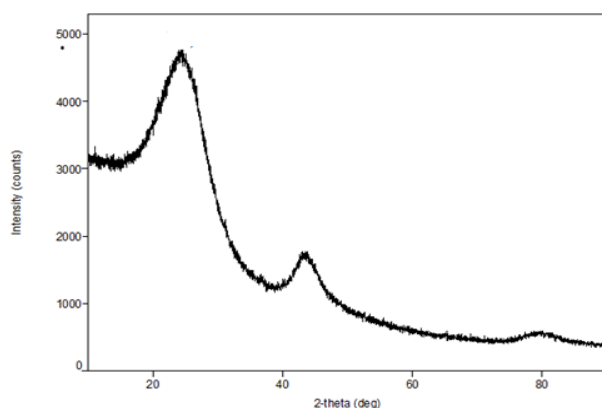


Figure 1. XRD of WAC.

3.1.2. FTIR analysis.

A single remarkable peak at 2349cm^{-1} is due to O in CO_2 . So, the combined mechanism of hydration followed by dissociation reactions may be suggested as follows in Figure 2.

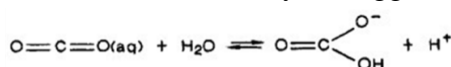


Figure 2. Hydration reaction of CO_2 .

According to Burke *et al.*, different functional groups present on typical carbon surfaces are carbonyls, hydroxyls, esters or carboxylic acids, and 60-70% of the total oxygen-containing functional groups is from $-\text{C}-\text{O}^-$ group [17]. The reaction between negatively charged adsorbent and the cationic dye may be accelerated because of the electrostatic force of attraction. The OH group provided by CO_2 in aqueous solution may also form hydrogen bonds (shown as dotted lines) with the highly electronegative N atoms of MB and MG, as shown in Figure 3.

3.1.3. Point of zero charge (pzc).

The charge on the adsorbent surface is described by pzc. At lower pH, i.e., below pzc, the surface of adsorbent becomes positively charged, and at higher pH compared to pzc the adsorbent surface becomes negatively charged. According to Figure 4, pzc of WAC is 6, and

the adsorbates under consideration are cationic dyes. So, at pH more than 6, dye adsorption should be favorable compared to lower pH.

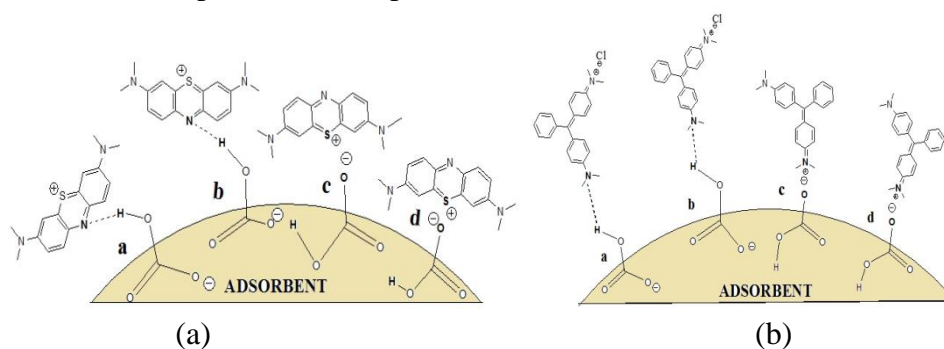


Figure 3. Probable mechanism of bond formation of WAC with (a) MB and (b) MG.

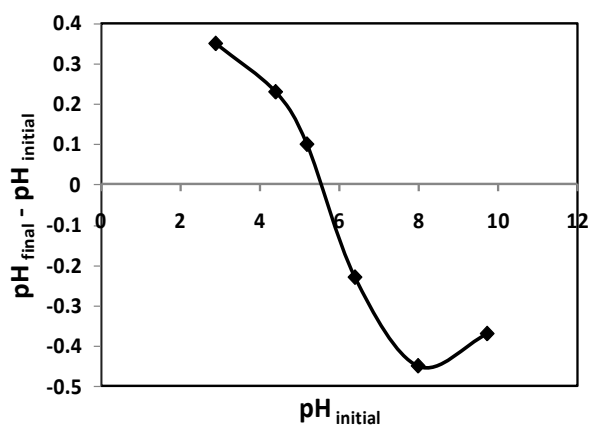


Figure 4. Determination of pzc of WAC.

3.1.4. Other physicochemical parameters.

The pH, % moisture content, % loss of mass on the ignition, density, and surface area were found to be 6.2, 5.5, 72.3, 1.11 g/cm³, and 75.2 m²/g, respectively. The pH is comparable to that of other reported activated carbon (pH = 6–7). Density is higher compared to that of commercial activated carbon, i.e., 0.5 g/cm³. Higher density leads to higher filtering ability. The surface area is also comparable to that of other reported carbon compounds [18].

3.2. Effect of different parameters.

3.2.1. Effect of contact time.

Time dependency of adsorption is an important parameter in adsorption experiments, and the same was investigated for the removal of MB and MG from aqueous solution using WAC. 50ml of 500mg/L dye solution with 1g of WAC was agitated up to 240 minutes. Samples at different time intervals were withdrawn and were analyzed for dye concentrations. The result is shown in Figure 5. From the graph, it is observed that 60 and 120 minutes are the optimum contact times for MB and MG adsorption, respectively. As in other adsorption studies here also the initial rate of adsorption is faster because of the free availability of active sites at the beginning. As the active sites gradually occupied by dye molecules, the rate of adsorption decreases, and the percentage of adsorption remain constant after equilibrium is achieved. The same trend has also been observed by Ghosh *et al.* and others [19].

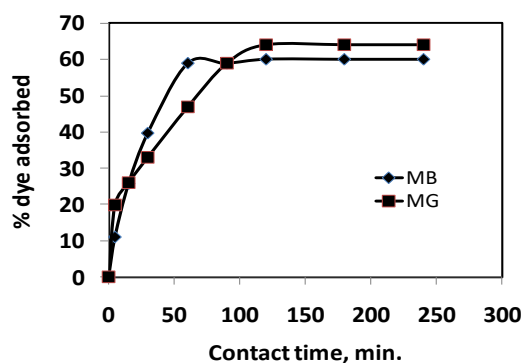


Figure 5. Effect of contact time on adsorption.

3.2.2. Effect of pH.

The adsorbate and adsorbent properties greatly depend on solution pH. Therefore, the effect of pH on adsorption of MB and MG by WAC over a wide pH range (2.5 – 7) was studied. Figure 6 shows the effect of pH on the said adsorption. Both MB and MG are cationic dyes and are positively charged in aqueous solution. The pzc of WAC is 6, as shown in Figure 4. So, it is expected that at low pH adsorption should be less, and at higher pH (after pH 6) it should be more. From the figure also, it is observed that adsorption increases slowly with increasing pH. However, the dye adsorption on various adsorbents is not only due to electrostatic force of attraction, but the additional contribution of other attractive forces like hydrophobic-hydrophilic interaction and hydrogen bonding should also be taken into consideration [20].

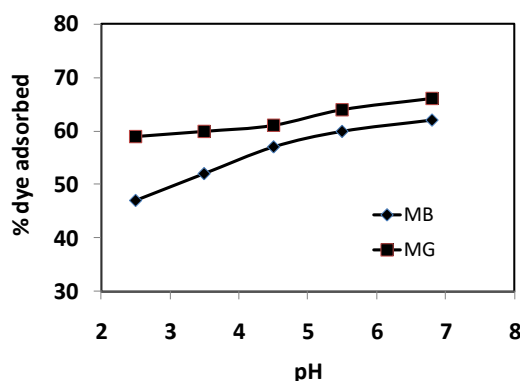


Figure 6. The effect of pH variation on adsorption.

3.2.3. Effect of adsorbent dose.

Adsorbent doses for the adsorption studies were varied (4 to 40 g/L), keeping other parameters constant. Figure 7 shows the result. It has been observed that adsorption percentage increases with an increase of adsorbent dose, and at 40 g/L adsorbent dose, almost complete removal of both MB and MG takes place. This is due to the availability of more surface area with the increase of adsorbent concentration. Dye uptakes, mg/g decreases with the increase of adsorbent dose, which is in accordance with the other reported literature [21].

3.2.4. Effect of dye concentration.

Dye (Both MB and MG) concentrations were varied from 100-700 mg/L while other adsorption parameters were kept unchanged. The % of dye removal decreases with an increase of dye concentration, whereas uptake, mg/g increases up to 400, and 500 mg/L dye concentration for MB and MG respectively, and thereafter dye uptakes were constant. The

result is shown in Figure 8. Because at higher dye concentration, the adsorbate:adsorbent ratios are high, and the probabilities of interaction between them become more leading to higher dye uptake. In addition, at higher adsorbate concentration, the electrostatic repulsion between positive charges of dye molecules results in the decrease of the adsorption percentage [22]. After the attainment of equilibrium, the availability of active sites towards dye is constant. Therefore, the rate of adsorption becomes constant. Even if the dye concentration is increased, therefore no further change in adsorption is observed after that.

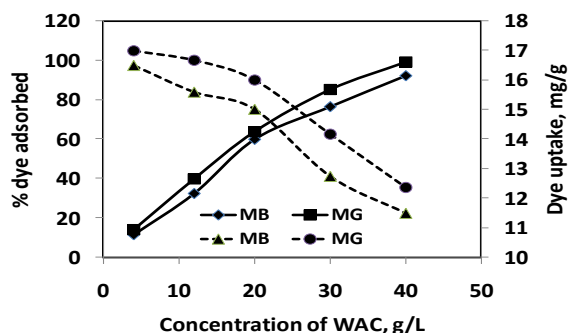


Figure 7. Effect of WAC concentration variation on % of adsorption (solid lines) and uptake (dotted lines).

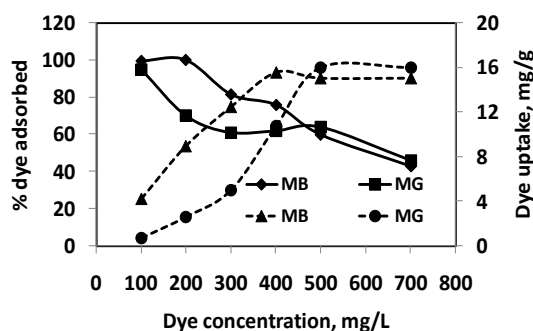


Figure 8. Effect of dye concentration variation on % of adsorption (solid lines) and uptake (dotted lines).

3.2.5. Effect of temperature.

The temperature of the system was changed from 30-60°C, whereas other adsorption parameters were kept constant. The effect of temperature on dye adsorption is shown in Figure 9. It has been seen from the figure that the dye adsorption on WAC is endothermic in nature, i.e., both MB and MG adsorption increases with the increase of temperature. It may be due to the opening of pore size and activation of the sorbent surface at a higher temperature. Three thermodynamic parameters such as ΔH , ΔS , and ΔG were calculated using the formula described in the experimental section, and the values are given in Table 3. The positive ΔH value (63.9 and 130 kJ/mol for MB, and MG, respectively) also indicates the endothermic nature of the adsorption process. The positive ΔS indicate the affinity of MB and MG dyes towards WAC surface and spontaneous nature of MB and MG adsorption on WAC surface. As we already know ΔG is positive for non-spontaneous process and negative for a spontaneous process. From Table 3, it is observed that out of four studied temperatures, MB adsorption is non-spontaneous at 303 and 313K and spontaneous at 323 and 333K. Similarly, MG adsorption on WAC at 303, 313, and 323 K are non-spontaneous, and at 333K, it is spontaneous.

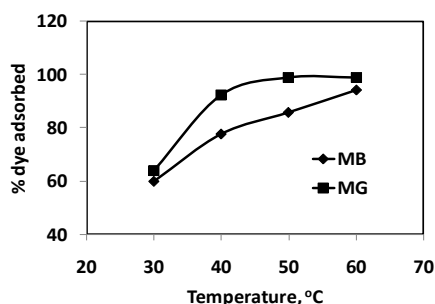


Figure 9. Effect of temperature on % of dye adsorption.

3.3. Adsorption isotherms and kinetics.

The interaction between adsorbate and adsorbent can be explained well by different isotherm models. Different isotherm models are Langmuir, Freundlich, and Temkin, etc. These isotherm models were studied at constant pH and temperature with the variation of dye concentrations. Langmuir isotherm explains monolayer adsorption on the homogeneous surface considering no interaction between the adjacent adsorbed molecules, whereas Freundlich isotherm explains multilayer adsorption on the heterogeneous adsorbent surface. The linear forms of Langmuir and Freundlich isotherm equations, along with their details, are given in Table 2.

Table 3. Different isotherms and kinetics parameters.

Name of the isotherms and kinetics	Parameters					
Langmuir isotherms	b(L/mg) 0.29 (MB) 0.015 (MG)	q _m (mg/g) 15.38 (MB) 18.87 (MG)	R _L 0.005–0.03 (MB) 0.09-0.4 (MG)	R ² 0.99 (MB) 0.91 (MG)		
Freundlich isotherms	n 7.35(MB) 3.36 (MG)	K (mg/g) 7.26 (MB) 2.65 (MG)		R ² 0.77 (MB) 0.85 (MG)		
Temkin isotherm	A _T (L/g) 338 (MB) 268 (MG)	B 1.33 (MB) 2.7 (MG)	b(J/mol) 1894.1 (MB) 933.01 (MG)	R ² 0.85 (MB) 0.74 (MG)		
Pseudo first order model	k ₁ (min ⁻¹) 0.05 (MB) 0.025 (MG)	q _e (mg/g) 15.81 (MB) 14.93 (MG)		R ² 0.91 (MB) 0.96 (MG)		
Pseudo second order model	k ₂ (g/mg.min) 0.003 (MB) 0.06 (MG)	q _e (mg/g) 16.67 (MB) 17.5 (MG)		R ² 0.99 (MB) 0.97 (MG)		
Morris-Weber equation	R _{id} (mg/g/min ^{0.5}) 1.51 (MB) 1.43 (MG)			R ² 0.94 (MB) 0.99 (MG)		
Thermodynamic parameters	ΔH (kJ/mol) 63.9 (MB) 130.0 (MG)	ΔS (J/mol.K) 214.08 (MB) 436.4 (MG)	ΔG (kJ/mol)		R ² 0.99 (MB) 0.88 (MG)	
			T, K	MB		MG
			303	3.3		8.8
			313	1.3		4.8
			323	-0.7		0.8
333	-2.7	-3.2				

The constants of both the isotherms along with R² values are given in Table 3. R² values for Langmuir isotherm is greater than that of Freundlich for both MB and MG adsorption. It indicates uniformly distributed monolayer coverage of both the dyes on the adsorbent WAC surface. The experimental maximum adsorption capacity (16.5 and 17mg/g) also matches well with Langmuir maximum adsorption capacity (15.38 and 18.87mg/g) for MB and MG, respectively.

The separation parameter (R_L) values derived from Langmuir’s constant b , as shown in Table 3, lie in the range 0 -1 also indicate favorable nature of both MB and MG dye adsorption on WAC surface. Temkin is another isotherm model that assumes that the heat of adsorption of all the molecules decreases linearly with the increase in coverage of the adsorbent surface, and during that, adsorption binding energy is distributed uniformly up to certain binding energy. Good correlation coefficients for Temkin’s isotherm, as shown in Table 3 show that it is obeyed well during MB and MG adsorption on WAC. A_T is the equilibrium binding constant corresponds to maximum binding energy and was found to be 338 and 268 L/g for MB and MG, respectively. B is another Temkin’s constant, which is related to the heat of sorption value b and $B = RT/b$. Here R is the universal gas constant, and T is the absolute temperature. For MB and MG, b was found to be 1894.1 and 933.01 J/mol, respectively, which indicates the physicochemical nature of the sorption process [23].

The study of adsorption kinetics for any adsorption process is very much essential as it gives us an idea about the rate and mechanism of adsorption reactions. Among all the kinetic models, pseudo-first and pseudo-second-order kinetics are the most important. So, experimental data were tested with both of these models. Higher R^2 values in the case of pseudo-second-order kinetics indicate that MB and MG adsorption on WAC is chemisorption in nature. The pseudo-second-order rate constants for MB and MG adsorption on WAC were found to be 0.003 and 0.06 g/mg.min, respectively. The data were tested with the Morris-Weber equation as well to know the nature of diffusion of adsorbate particles through the adsorbent. The straight lines obtained pass nearly through the origin for both MB and MG. So, mass transfer during the initial and final stages of adsorption is almost the same. This confirms that both MB and MG adsorption on WAC surface are a single step process. A good correlation coefficient for the plot indicates that during adsorption, intraparticle diffusion also takes place.

3.4. Comparison with other low cost adsorbents.

Langmuir maximum MB and MG uptakes on WAC are found to be 15.38 and 18.87mg/g, respectively, as shown in Table 3. These values are comparable to the uptakes of the same dyes by other reported low-cost adsorbents, as follows in Table 4.

Table 4. Comparison of MB and MG uptakes (q_m) by WAC with other low-cost adsorbents.

Adsorbents	Methylene Blue (MB)		Adsorbents	Malachite Green (MG)	
	q_m , mg/g	References		q_m , mg/g	References
Kaolinite clay	15.6	[24]	Carbon nanotubes	11.73	[29]
Orange peel	18.6	[25]	Rice husk	6.5	[30]
Sawdust carbon	12.49-51.4	[26]	Talc (silicate material)	20.9	[31]
Sunflower oil cake	16.4	[27]	Lignin	31	[32]
H ₂ SO ₄ treated waste fruit of <i>Rapanea ferruginea</i>	33	[28]	Stem of Solanum tuberosum	27.0	[33]
Waste Activated Carbon (WAC)	15.38	Present study	Waste Activated Carbon (WAC)	18.87	Present study

4. Conclusions

The carbon waste collected from domestic water filter (WAC) can remove cationic dyes methylene blue (MB) and malachite green (MG) effectively from the synthetic aqueous solution. The novelty of this work is the optimization of sorption conditions for MB and MG adsorption on new low-cost material and evaluation of the corresponding adsorption

mechanism. The optimum contact time for MB and MG adsorptions are 60 and 120 minutes, respectively. The adsorption percentage increases slowly with the increase of pH from 2.5 to 7. The positive enthalpy change suggests the reaction to be endothermic. The reactions are spontaneous at a higher temperature. Langmuir is the better-suited isotherm compared to Freundlich and Langmuir maximum uptake for MB and MG are found to be 15.38 and 18.87mg/g, respectively. Pseudo-second-order kinetics is obeyed well compared to pseudo-first-order with rate constants equal to 0.003 and 0.06g/mg.min for MB and MG, respectively. Temkin's maximum binding energies are found to be 338 and 268 L/g for MB and MG, respectively, which indicates the physicochemical nature of the adsorption process. Intra particle diffusion is the rate-limiting stage. The present small scale batch adsorption process can be applied to a large continuous flow column study for the removal of dye from real polluted water.

Funding

This research received no external funding.

Acknowledgments

The authors pay their gratitude and are indebted to The President, Siksha 'O' Anusandhan (Deemed to be University), Bhubaneswar, for providing the full facility for research activities and for granting permission to publish this paper. The authors also thank Mr. Biswaprakash Sarangi, research scholar of their department, for his help in drawing the figures.

Conflicts of Interest

The authors declare no conflict of interest.

References

1. Hossain, M.A.; Ali, M.M.; Islam, T.S.A. Comparative adsorption of Methylene Blue on different lowcost adsorbents by continuous column process. *International Letters of Chemistry, Physics and Astronomy***2018**, *77*, 26-34, <https://doi.org/10.18052/www.scipress.com/ILCPA.77.26>.
2. Said, B.; Souad, M.; Ahmed, E.H. Classifications, properties, recent synthesis and applications of azo dyes. *Heliyon***2020**, *6*, <https://doi.org/10.1016/j.heliyon.2020.e03271>.
3. Mohd., R.; Othman, S.; Rokiah, H., Anees A. Adsorption of methylene blue on low-cost adsorbents: A review. *Journal of Hazardous Materials***2010**, *177*, 70–80, <https://doi.org/10.1016/j.jhazmat.2009.12.047>.
4. Srivastava, S.; Sinha, R.; Roy, D. Toxicological effects of malachite green. *Aquat Toxicol.* **2004**, *66*, 319-29, <https://doi.org/10.1016/j.aquatox.2003.09.008>.
5. MegatHanafiah, M.A.K.; MohdJamaludin, S.Z.; Khalid, K.; Ibrahim, S. Methylene blue adsorption on aloe vera rind powder: kinetics, isotherm and mechanisms. *Nature. Environ. Pollut. Technol.***2018**, *17*, 1055–1064.
6. Massoud, K.; Mojtaba, S.; Sahar M. Removal of Dyes from the Environment by Adsorption Process. *Chemical and Materials Engineering* **2018**, *6*, 31-35, <https://doi.org/10.13189/cme.2018.060201>.
7. Achary, P.G.R.; Ghosh, M.R.; Mishra, S.P. Insights into the modeling and application of some low cost adsorbents towards Cr(VI) adsorption. *Materials Today Proceedings***2020**, <https://doi.org/10.1016/j.matpr.2020.01.433>.
8. Shabaan, O.A.; Jahin, H.S.; Mohamed, G.G. Removal of anionic and cationic dyes from wastewater by adsorption using multiwall carbon nanotubes. *Arabian J of Chemistry***2020**, *13*, 4797-4810, <https://doi.org/10.1016/j.arabjc.2020.01.010>.
9. Saleem, J.; Shahid, U.; Hijab, M. Production and applications of activated carbons as adsorbents from olive stones. *Biomass Conv. Bioref.* **2019**, *9*, 775–802, <https://doi.org/10.1007/s13399-019-00473-7>.
10. Ani, J.U.; Akpomie, K.G.; Okoro, U.C.; Aneke, L.E.; Onukwuli, O.D.; Ujam, O.T. Potentials of activated carbon produced from biomass materials for sequestration of dyes, heavy metals, and crude oil components from aqueous environment. *Appl Water Sci.* **2020**, *10*, <https://doi.org/10.1007/s13201-020-1149-8>.

11. Bordoloi, N.; Dey, M.D.; Mukhopadhyay, R.; Katak, R. Adsorption of Methylene blue and Rhodamine B by using biochar derived from *Pongamia glabra* seed cover. *Water Sci. Technol.* **2018**, *77*, 638–646, <https://doi.org/10.2166/wst.2017.579>.
12. Raval, N.P.; Shah, P.U.; Shah, N.K. Malachite green “a cationic dye” and its removal from aqueous solution by adsorption. *Appl Water Sci.* **2017**, *7*, 3407–3445, <https://doi.org/10.1007/s13201-016-0512-2>.
13. Mishra, S.P.; Achary, P.G.R.; Das, M. Adsorption of Cu(II) by Used Aquaguard Carbon (UAC). *Journal of Chemical and Pharmaceutical Research* **2012**, *4*, 1207–1216.
14. Mishra, S.P.; Ghosh, M.R. Use of silver impregnated activated carbon (SAC) for Cr(VI) removal. *Journal of Environmental Chemical Engineering*, **2020**, *8*, <https://doi.org/10.1016/j.jece.2019.103641>.
15. Ghosh, M.R.; Mishra, S.P. Adsorption of Cr(VI) by using HCl modified *Lagenariasicerari* peel (HLSP). *J. Mater. Environ. Sci.* **2016**, *7*, 3050–3060.
16. Golkarian, A.R.; Jabbarzadeh, M. The density effect of van der Waals forces on the elastic module in graphite layers. *Comput. Mater. Sci.* **2013**, *74*, 138–142, <https://doi.org/10.1016/j.commatsci.2013.03.026>.
17. Asadinezhad, A.; Lehoc, M.; Saha, P.; Mozetic, M. Recent progress in surface modification of polyvinyl chloride. *Materials* **2012**, *5*, 2937–2959.
18. Contescu, C.I.; Adhikari, S.P.; Gallego, N.C.; Evans, N.D.; Bliss, B.E. Activated carbons derived from high-temperature pyrolysis of lignocellulosic biomass. *J. of Carbon Research*. **2018**, *4*, <https://doi.org/10.3390/c4030051>.
19. Ghosh, M.R.; Mishra, S.P. Effect of Co-ions on Cr(VI) and F⁻ Adsorption by Thermally Treated Bauxite (TTB). *Arab J Sci Eng.* **2017**, *42*, 4391–4400, <https://doi.org/10.1007/s13369-017-2472-8>.
20. Fangwen, L.I.; Xiaoi, W.U.; Songjiang, M.A.; Zhongjian, X.U.; Wenhua, L.I.U.; Fen, L.I.U. Adsorption and desorption mechanisms of methylene blue removal with iron-oxide coated porous ceramic filter. *J. Water Resource and Protection* **2009**, *1*, 1–57, <https://doi.org/10.4236/jwarp.2009.11006>.
21. Kristanti, R.A.; Hadibarata, T.; Al Qahtani, H.M.S. Adsorption of bisphenol A on oil palm biomass activated carbon : Characterization, isotherm, kinetic and thermodynamic studies. *Biointerface Research in Applied Chemistry* **2019**, *9*, 4217–4224, <https://doi.org/10.33263/BRIAC95.217224>.
22. Mohammed, A.A.; Mohammed, S.A.; Zaid, A.A. Sorption of methylene blue onto the biomass of date palm seeds: kinetic study. *Biointerface Research in Applied Chemistry* **2018**, *8*, 3583–3589.
23. Kuang, Y.; Zhang, X.; Zhou, S. Adsorption of Methylene Blue in water onto activated carbon by surfactant modification. *Water* **2020**, *12*, <http://dx.doi.org/10.3390/w12020587>.
24. Mukherjee, K.; Kedia, A.; Rao, K.J.; Dhir, S.; Paria, S. Adsorption enhancement of methylene blue dye at kaolinite clay-water interface influenced by electrolyte solutions. *RSC Advances* **2015**, *5*, 30654–30659, <https://doi.org/10.1039/C5RA03534A>.
25. Hee-Jeong, C.; Sung-When, Y. Biosorption of methylene blue from aqueous solution by agricultural bioadsorbent corncob. *Environ. Eng. Res.* **2019**, *24*, 99–106, <https://doi.org/10.4491/eer.2018.107>.
26. Corda, N.C.; Kini, M.S. A review on adsorption of cationic dyes using activated carbon. *MATEC Web of Conferences* **2018**, *144*, <https://doi.org/10.1051/mateconf/201814402022>.
27. Rafatullah, M.; Sulaiman, O.; Hashim, R.; Ahmad, A. Adsorption of methylene blue on low-cost adsorbents: A review. *J Hazard Mater.* **2010**, *177*, 70–80, <https://doi.org/10.1016/j.jhazmat.2009.12.047>.
28. Chahm, T.; Martins, B.A.; Rodrigues, C.A. Adsorption of methylene blue and crystal violet on low-cost adsorbent: waste fruits of *Rapanea ferruginea* (ethanol-treated and H₂SO₄-treated). *Environ Earth Sci.* **2018**, *77*, <https://doi.org/10.1007/s12665-018-7681-2>.
29. Rajabi, M.; Mirza, B.; Mahanpoor, K.; Mirjalili, M.; Najafi, F.; Moradi, O.; Sadegh, H.; Shahryari-ghoshekandi, R.; Asif, M.; Tyagi, I.; Agarwal, S.; Gupta, V.K. Adsorption of malachite green from aqueous solution by carboxylate group functionalized multi-walled carbon nanotubes: Determination of equilibrium and kinetics parameters, *J. Ind. Eng. Chem.* **2016**, *34*, 130–138, <https://doi.org/10.1016/j.jiec.2015.11.001>.
30. Gündüz, F.; Bayrak, B. Synthesis and performance of pomegranate peel-supported zero-valent iron nanoparticles for adsorption of malachite green, *Desalin. Water Treat.* **2018**, *110*, 180–192, <https://doi.org/10.5004/dwt.2018.22185>.
31. Lee, Y.C.; Kim, J.Y.; Shin, H.J. Removal of malachite green (MG) from aqueous solutions by adsorption, precipitation and alkaline fading using talc. *Sep. Sci. Technol.* **2013**, *48*, 1093–1101, <https://doi.org/10.1080/01496395.2012.723100>.
32. Lee, S.; Park, J.; Kim, S. Sorption behavior of malachite green onto pristine lignin to evaluate the possibility as a dye adsorbent by lignin. *Appl Biol Chem.* **2019**, *62*, <https://doi.org/10.1186/s13765-019-0444-2>.
33. Thirumorthy, K.; Krishna, S.K. Removal of cationic and anionic dyes from aqueous phase by Ball clay –Manganese dioxide nanocomposites, *J. Env. Chem. Eng.* **2020**, *8*, <https://doi.org/10.1016/j.jece.2019.103582>.